

## DETAILED ANALYSIS OF AMORPHOUS SILICON PASSIVATION LAYERS DEPOSITED IN INDUSTRIAL IN-LINE AND LABORATORY-TYPE PECVD REACTORS

Marc Hofmann<sup>1</sup>, Christian Schmidt<sup>1</sup>, Norbert Kohn<sup>1</sup>, Dieter Grambole<sup>2</sup>, Jochen Rentsch<sup>1</sup>, Stefan Glunz<sup>1</sup> and Ralf Preu<sup>1</sup>

<sup>1</sup>Fraunhofer Institute for Solar Energy Systems (ISE)  
Heidenhofstrasse 2, D-79110 Freiburg, Germany  
phone: +49 761-4588-5614; fax: +49 761-4588-9250  
email: marc.hofmann@ise.fraunhofer.de

<sup>2</sup>Forschungszentrum Dresden-Rossendorf,  
Bautzner Landstr. 128, 01328 Dresden, Germany

**ABSTRACT:** Amorphous silicon (a-Si) layers for the passivation of p-type silicon wafer surfaces are investigated. The first main topic is the thermal stability of a-Si passivation. Here, an improved thermal stability in annealing (400 °C) and firing processes (wafer temp. 550 °C) could be achieved by stacking a-Si layers with PECVD SiO<sub>x</sub> layers of different thickness. Hydrogen depth profiling using nuclear reaction analysis shows a hydrogen concentration of 11 at% in the bulk of the a-Si. After firing of single layer a-Si samples a hydrogen concentration peak at the a-Si / c-Si interface could be observed. The second major topic of this paper is the deposition of a-Si layers using an industrial-type inline PECVD reactor. Excellent surface passivation (>1 ms on 1 Ohm cm FZ wafers) can be reported. These a-Si layers are further characterised using FTIR and spectroscopic ellipsometry.

**Keywords:** a-Si, annealing, CVD based deposition, lifetime, PECVD

### 1 INTRODUCTION

In previous publications, hydrogenated amorphous silicon (a-Si:H, in short: a-Si), deposited by PECVD (plasma enhanced chemical vapour deposition), has been shown to be an excellent means for passivating the surfaces of silicon wafers. Especially for the rear of PERC (passivated emitter and rear cell, [1]) type solar cells its capability has been shown by different researchers [2-4]. When stacking the amorphous silicon layer with an additional PECVD silicon oxide layer (SiO<sub>x</sub>) additional benefits could be gained [4]. Fraunhofer ISE has developed and patented a process for fabricating local rear contacts for PERC cells in a very quick manner for high-efficiency applications by laser processing ("laser fired contacts", LFC, [5]).

### 2 THERMAL STABILITY

#### 2.1 Introduction and experimental

As the thermal stability of amorphous silicon seems to be the most obstructive part in the transfer of the amorphous silicon passivation layers into industrial production, an investigation has been performed on this topic. Silicon wafers with the following properties were used: float zone, p-type, boron doped, 1 Ω cm, 250 μm thick, shiny etched surfaces.

The wafers were processed in the following manner: The first side of the wafer was cleaned by a plasma etching step using a microwave remote plasma with only SF<sub>6</sub> and Ar as gas flow. Next, the samples were transported through air and the deposition of a-Si was done. Most samples received an additional deposition of a SiO<sub>x</sub> layer in varying thickness (50 nm, 100 nm, 200 nm, 500 nm) on top of the a-Si film. The a-Si deposition took place using a gas mixture of silane (SiH<sub>4</sub>) and hydrogen (H<sub>2</sub>) with a plasma excitation frequency of 13.56 MHz in a direct plasma reactor. The SiO<sub>x</sub> deposition was done in the same plasma chamber using the same excitation frequency but changing the gas mixture to silane (SiH<sub>4</sub>)

and nitrous oxide (N<sub>2</sub>O).

For the second side of the wafer the same procedure was applied (plasma etch + deposition of a-Si and SiO<sub>x</sub>). After measuring the minority carrier lifetime using the QSSPC (quasi-steady state photoconductance) method [6], the samples were attributed to an annealing step in forming gas (95% N<sub>2</sub>, 5% H<sub>2</sub>) at 400 °C for 5 min (plus 10 min of ramping up the temperature). Then, the minority carrier lifetime of the samples was measured again, followed by the next annealing step and so on. Please see the process flow chart in figure 1.

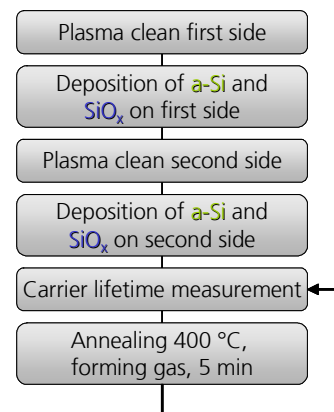


**Figure 1:** Process sequence of the investigation on thermal stability.

The final sample structure can be found in figure 2.

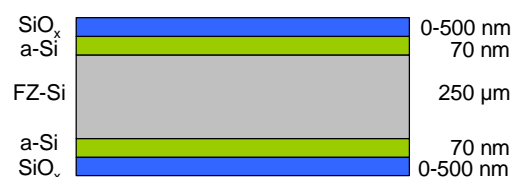


**Figure 2:** Sample structure of the investigation on thermal stability.

### 2.2 Results

Initially (as-deposited), all samples showed an excellent surface passivation with lifetimes in the range of 900  $\mu\text{s}$  to 1600  $\mu\text{s}$ . As the maximum bulk lifetime of these samples can be calculated to 2300  $\mu\text{s}$  when only Auger recombination is assumed with the Auger model by Glunz and Rein [7] the surfaces must be at a very well passivated state. Surface recombination velocities in the range of 9 cm/s to 3 cm/s can be calculated using the equation of Nagel et al. [8]. No significant difference between the single-layer a-Si and the double layer a-Si + SiO<sub>x</sub> could be observed.

After annealing for 5 min in forming gas at 400 °C most lifetime results were quite stable. Exception: the samples with lifetimes of approx. 900  $\mu\text{s}$  in the as-deposited state (samples with SiO<sub>x</sub> thickness 50 nm and 200 nm) improved significantly to 1100  $\mu\text{s}$  to 1300  $\mu\text{s}$ . The samples with single layer a-Si passivation degraded a bit to approx. 900  $\mu\text{s}$ .

With increasing annealing time all lifetime values degraded.

A stronger degradation could be found for the single layer a-Si passivated sample. After 30 min an approximate lifetime of 200  $\mu\text{s}$  could be measured.

The stack layer samples (a-Si + SiO<sub>x</sub>) generally showed a better thermal stability compared to the single layer (a-Si) samples. No clear dependence could be found for the thickness of the SiO<sub>x</sub> layer in the investigated thickness range. In figure 3 the effect of the described annealing on the effective minority carrier lifetime can be found.

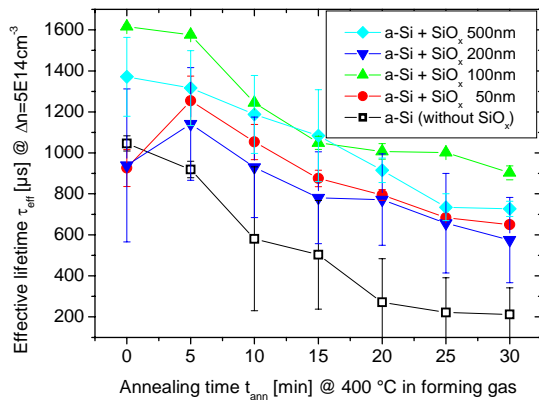


**Figure 3:** Effective minority carrier lifetime vs. the annealing time of the samples in forming gas at 400 °C.

For the annealing of finished solar cells with local rear contacts typically a duration of approx. 10 min is sufficient which leaves the lifetime on a very high level.

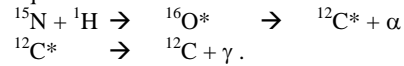
### 3 HYDROGEN DEPTH PROFILING

#### 3.1 Nuclear Reaction Analysis (NRA)

Hydrogen is suspected to play a crucial role in the passivation effect. Therefore, the status and change in hydrogen concentration in the passivation layer after a thermal treatment is of great interest.

Nuclear Reaction Analysis (NRA) measurements have been performed in collaboration with the Forschungszentrum Rossendorf, Germany. NRA is based on a reaction between a nitrogen isotope <sup>15</sup>N which is accelerated to several MeV and a hydrogen atom <sup>1</sup>H in

the sample. The reaction only takes place when the nitrogen atom has a specific kinetic resonance energy (6.385 MeV). At a lower energy, no nuclear reaction will happen. At a higher energy, the nitrogen atom loses speed (energy) while passing through the first atomic layers of the film. When the nitrogen is decelerated to the resonance energy, the reaction will happen if there is a hydrogen atom to react with. The reaction of hydrogen and nitrogen will finally lead to a <sup>12</sup>C atom and an alpha and a gamma quantum that are radiated. The reaction equations are as follows



Counting the measured gamma quanta for a certain nitrogen kinetic leads to the hydrogen concentration and the depth profile [10].

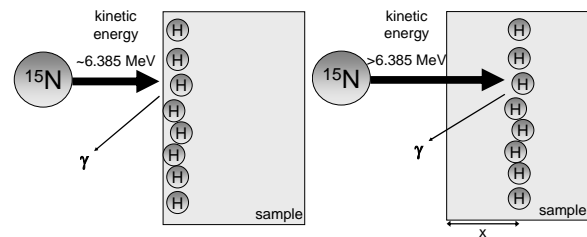


**Figure 4:** Measurement principle of the NRA technique (after [9]).

#### 3.2 Hydrogen profiles of single layer a-Si samples

The NRA measurements have shown a high hydrogen concentration in the as-deposited a-Si layer of approx. 11 at%. After annealing a slightly lower concentration of approx. 9 at% can be found. The shape of the hydrogen distribution within the a-Si layers is almost the same with a quite stable H concentration in the a-Si bulk, very low values in the c-Si bulk in the order of 0 to 1 at% and a quite strong decline at the interface. As the measuring method is averaging over 8 nm in depth and the measurement spot is approx. 2\*4 mm<sup>2</sup>, the measured signal always is an average value.

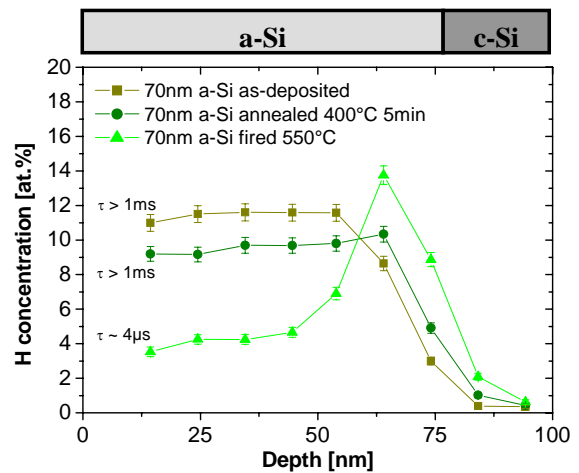


**Figure 5:** Hydrogen depth profile of a crystalline silicon substrate (c-Si) with amorphous silicon layer (a-Si) on top. Profiling at samples directly after deposition and with different post-deposition thermal treatments (annealing in forming gas at 400 °C for 5 min and firing in fast firing oven at a peak temperature of 550 °C for ~3 s).

The sample that was fired at a peak temperature of 550 °C (real wafer temperature) is strongly effected by the thermal processing. The a-Si bulk hydrogen content is lowered to approx. 4 at%. A strong hydrogen accumulation at the a-Si / c-Si interface could be observed with a peak hydrogen concentration of 14 at%. This accumulation typically leads to blistering at the a-Si/c-Si interface and depassivates the sample's surfaces. This effect is expected to enhance when accelerated temperatures or prolonged times are used.

### 3.3 Hydrogen profiles of a-Si/ SiO<sub>x</sub> stack layers

In section 2 an increased thermal stability of the amorphous silicon passivation could be observed when the a-Si layer was stacked with an additional PECVD SiO<sub>x</sub> layer. Therefore, the hydrogen depth profile of such a stack layer system is investigated as well.

In figure 6 the depth profiles of a single layer a-Si sample and a stack layer system can be found. Both samples have been fired at a sample temperature of 550 °C for approx. 3 s.

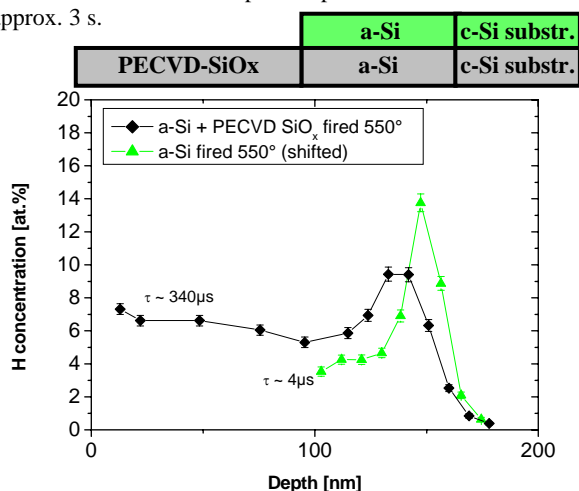


**Figure 6:** Hydrogen depth profile of a crystalline silicon substrate (c-Si) with a-Si (black) or a stack of a-Si + PECVD-SiO<sub>x</sub> (red) on top. For orientation a scheme of the layer systems can be seen above the graph indicating the different areas in the graph.

The most dominant observation is the decreased height of the hydrogen concentration peak at the a-Si / c-Si interface and the higher hydrogen concentration in the a-Si bulk compared to the single layer a-Si sample.

The samples' minority carrier lifetimes were approx. 340 µs (a-Si + SiO<sub>x</sub> stack system) and 4 µs (single layer a-Si passivation). A correlation between the hydrogen concentration at the a-Si / c-Si interface and the minority carrier lifetime seems to be possible.

Blistering was visible without magnification after higher firing temperatures at single layer a-Si samples. At 550 °C sample temperature the hydrogen clustering effect seems to be just starting.

## 4 A-SI DEPOSITION USING AN INDUSTRIAL IN-LINE PECVD REACTOR

### 4.1 Introduction

The deposition of high-quality passivating amorphous silicon in a small laboratory-type direct plasma PECVD reactor has been proved earlier [4]. For implementation of the a-Si passivation process it is necessary to transfer

the deposition process to high-throughput equipment. In our investigation a SiNA machine from Roth&Rau has been used (SiNA XS). This PECVD tool exhibits plasma excitation by microwaves that are introduced into the reactor by linear antennas. In our case two linear antennas in series were applied. Please find a photograph of our SiNA tool in figure 7.



**Figure 7:** Photograph of the Roth&Rau SiNA tool used for the deposition of a-Si layers using an industrial PECVD reactor within this investigation.

The Roth&Rau SiNA is typically used for the deposition of the anti-reflecting silicon nitride (SiN<sub>x</sub>:H) films used on standard industrial solar cells for the front side deposition. Therefore, it is a well-known tool that is available in many solar cell fabs around the globe.

### 4.2 Lifetime investigation

The first topic one is typically interested in is the surface passivation quality of a-Si layers deposited with the industrial PECVD tool. Therefore, high-quality silicon wafers with the following characteristics were used: float zone, p-type, boron doped, 1 Ω cm, 250 µm thick, shiny etched surfaces.

After cleaning the surfaces in a wet chemical RCA bath sequence, amorphous silicon has been deposited sequentially on both surfaces. Next, the minority carrier lifetimes were measured with the QSSPC technique leading to lifetimes up to >1 ms (<10 cm/s). Please find the lifetime result of one of the best samples in figure 8.

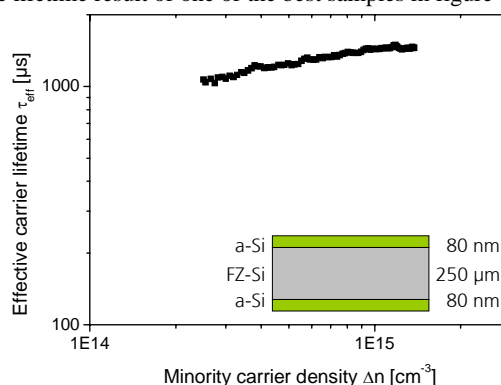


**Figure 8:** Effective minority carrier lifetime vs. the minority carrier density of one of the best samples with a-Si passivation deposited in the industrial in-line PECVD reactor and sample structure.

### 4.3 FTIR analysis

Fourier transformed infrared spectroscopy (FTIR) offers a means to characterise the composition of thin layers. In

our case a comparison between an a-Si layer deposited in our laboratory-type and our industrial-type PECVD reactor is performed. Its results can be found in figure 9.

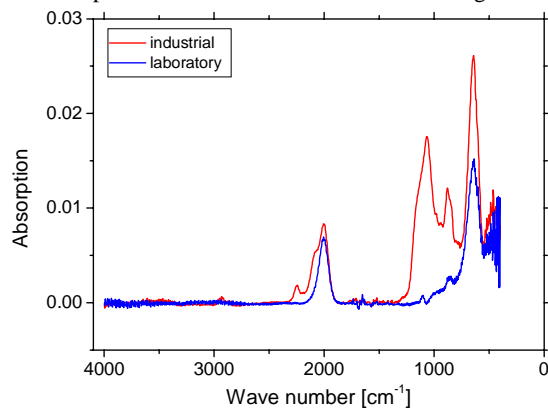


**Figure 9:** FTIR spectra of amorphous silicon layers deposited in a laboratory-type (blue) and an industrial-type PECVD reactor (red).

The thickness of the layers is approximately the same (lab: 70 nm, industr.: 85 nm). Therefore, the peak heights can directly be compared. The absorption peaks at  $2000\text{ cm}^{-1}$  is attributed to Si-H bonds. Hence, the Si-H bond density in both layers is approx. in the same order of magnitude.

In the wave number range around  $1000\text{ cm}^{-1}$  the absorption peaks correspond to Si-O and Si-N bonds. It seems clear that the a-Si layer deposited in the industrial-type PECVD reactor is contaminated with nitrogen and oxygen in a stronger way than the reference a-Si layer. This conclusion has been underlined by additional ERDA (elastic recoil detection analysis) measurements. Nevertheless, this does not lower the surface passivation properties significantly.

#### 4.4 Spectroscopic ellipsometry

Further characterisation of the a-Si layer has been performed using spectroscopic ellipsometry. A J.A.Woollam M-2000 ellipsometre with a spectroscopic range of 250 nm to 1000 nm has been used.

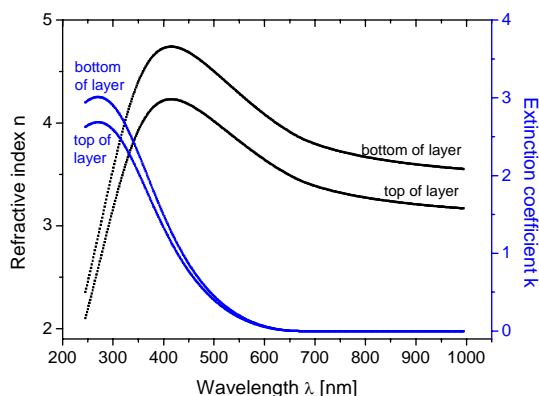


**Figure 10:** Refractive index  $n$  and extinction coefficient  $k$  vs. the wavelength of the a-Si layer deposited with the in-line industrial-type PECVD reactor.

The best fit for the data could be achieved when a linear gradient in the refractive index  $n$  and the extinction coefficient  $k$  has been assumed. Please see figure 10.

The ellipsometric results show typical values for a-Si layers.

#### CONCLUSION

In this paper an improved thermal stability of amorphous silicon could be demonstrated for stacks of a-Si and PECVD-SiO<sub>x</sub> at  $400\text{ °C}$  annealing temperature and in a firing step with a peak wafer temperature of  $550\text{ °C}$ . Hydrogen depth profiling showed a hydrogen concentration of approx. 11 at% in the a-Si bulk after deposition. This value decreases with increasing thermal treatment temperature. A hydrogen concentration peak at the a-Si / c-Si interface has been observed for single layer a-Si samples after firing at  $550\text{ °C}$ . These samples exhibit a very low passivation quality compared to the excellent passivation after deposition or annealing. With an additional SiO<sub>x</sub> layer good lifetimes even after firing could be achieved.

Excellent surface passivation could be reported for a-Si layers deposited in an industrial-type inline PECVD reactor. These a-Si layers exhibit an increased absorption in FTIR measurements which are attributed to N and O contamination. Spectroscopic ellipsometry shows that (i) refractive indices can be reported that are typical for a-Si and (ii) a gradient in the refractive index and extinction coefficient is observed.

#### ACKNOWLEDGEMENTS

The authors would like to thank A. Leimenstoll for clean room processing.

This work was supported by the EU funded project „Crystal Clear“ under the project number SES6-CT2003-502583.

#### REFERENCES

- [1] A.W. Blakers, J. Zhao, A. Wang, A.M. Milne, X. Dai and M.A. Green, Proceedings of the 9th European Photovoltaic Solar Energy Conference, Freiburg, Germany (1989) 328.
- [2] M. Schaper, J. Schmidt, H. Plaquizit and R. Brendel, Progress in Photovoltaics: Research and Applications 13 (2005) 381.
- [3] W. Brendle, V.X. Nguyen, A. Grohe, E. Schneiderlöchner, U. Rau, G. Palfinger and J.H. Werner, Progress in Photovoltaics: Research and Applications (2006) in press.
- [4] M. Hofmann, S. Glunz, R. Preu and G. Willeke, Proceedings of the 21st European Photovoltaic Solar Energy Conference, Dresden, Germany (2006) 609.
- [5] E. Schneiderlöchner, R. Preu, R. Lüdemann and S.W. Glunz, Progress in Photovoltaics: Research and Applications 10 (2002) 29.
- [6] R.A. Sinton, A. Cuevas and M. Stuckings, Proceedings of the 25th IEEE Photovoltaic Specialists Conference, Washington DC, USA (1996) 457.
- [7] S.W. Glunz, D. Biro, S. Rein and W. Warta, Journal of Applied Physics 86 (1999) 683.
- [8] H. Nagel, C. Berge and A.G. Aberle, Journal of Applied Physics 86 (1999) 6218.
- [9] M. Schwickert, in Mathematisch-Naturwissenschaftliche Fakultäten, pp. 135, Georg-August-Universität, Göttingen 2002.
- [10] W. Rudolph, C. Bauer, K. Brankoff, D. Grambole, R. Grötzschel, C. Heiser and F. Herrmann, Nucl. Instr. and Meth. B15 (1986) 508.